Fractal Analysis of Pharmaceutical Particles by Atomic Force Microscopy

Tonglei Li[1] and Kinam Park[1,2]

Received March 11, 1998; accepted May 14, 1998

Purpose. Reliable methods are needed to characterize the surface roughness of pharmaceutical solid particles for quality control and for finding the correlation with other properties. In this study, we used fractal analysis to describe the surface roughness.

Methods. Atomic force microscopy (AFM) was used to obtain three-dimensional surface profiles. The variation method was used to calculate fractal dimensions. We have measured fractal dimensions of four granule samples, four powders, and two freeze-dried powders.

Results. A computer program was written to implement the variation method. The implementation was verified using the model surfaces generated by fractional Brownian motion. The fractal dimensions of most particles and granules were between 2.1 and 2.2, and were independent of the scan size we measured. The freeze-dried samples, however, showed wide variation in the values of fractal dimension, which were dependent on the scan size. As scan size increased, the fractal dimension also increased up to 2.5.

Conclusions. Fractal analysis can be used to describe surface roughness of pharmaceutical particles. The variation method allows calculation of reliable fractal dimensions of surface profiles obtained by AFM. Careful analysis is required for the estimation of fractal dimension, since the estimates are dependent on the algorithm and the digitized model size (i.e., number of data points of the measured surface profile) used. The fractal dimension of pharmaceutical materials is also a function of the observation scale (i.e., the scan size) used in the profile measurement. The multi-fractal features and the scale-dependency of fractal dimension result from the artificial processes controlling the surface morphology.

KEY WORDS: fractal analysis; fractal dimension; atomic force microscope; surface roughness; surface morphology; surface topography.

INTRODUCTION

Solid dosage forms have been used as the major means to deliver therapeutic compounds (1). The manufacturing of solid dosage forms requires processing of pharmaceutical solid particles including powders and granules. Characterization of the particle size, shape and surface morphology is critical for quality control and assurance of the physicochemical properties of final products. Although the methods for characterizing particle size (2) and particle shape (3) are available, additional efforts are needed to study surface roughness or irregularity. Surface roughness is known to play an important role in the manufacturing processes and to affect the physicochemical properties of the drug products (3–7). The surface roughness of particles is influenced by manufacturing processes, molecular reactions, and microscopic processes occurring during production. Thus, characterization of surface roughness of a pharmaceutical material not only helps predict its physicochemical properties but also provides a reference to reflect any mechanical or physicochemical process involved in the surface formation.

Characterization of surface roughness involves two steps: instrumental measurement and quantification of the surface roughness. In our study, an atomic force microscope (AFM) was used to measure the surface topography. AFM allows measurements of the surface profiles at the nanometer scale. Studying the surface roughness at nano- or micro-scale can add more information to finding relationships between the surface morphology and the surface properties. Quantifying the surface roughness includes two attributes: roughness heights and lateral dimensions (8). It has been a tradition to use roughness heights to represent surface roughness. These include arithmetic mean surface roughness, root mean square roughness, average peak to valley height between five highest peaks and five deepest valleys within the sampling length, and skewness (9,10). These parameters, however, were known to be poor representations of surface roughness (9,10). Another attribute of surface roughness, lateral dimension, describes how frequently the surface height changes. It is conceptually simple, but finding a good quantitative representation of the lateral dimension in practice is not easy. The power spectrum method describes a measured surface profile as a superposition of different waveforms by applying Fourier transform methods (11,12). This method is able to describe the lateral dimensions of surface texture as well as the roughness heights. However, it is not a simple or straightforward representation of surface roughness and is difficult to directly correlate the power spectrum to the properties of solid materials.

Fractal dimension is able to represent lateral dimension. In 1977, Mandelbrot established the basic theory of fractal analysis (13). Since then, this concept has been studied in depth. For a three-dimensional surface, the fractal dimension is a decimal number between 2 and 3. It describes the spacing-filling ability. The higher the value, the rougher the surface. The surface/interface topographies of all materials are fractals at the molecular level (14). It has been demonstrated that the fractal analysis, a methodology to compute the fractal dimension of an object with various algorithms, is an ideal tool to evaluate surface irregularity (8,15,16). In our study, we have chosen the variation method to calculate fractal dimension. We report a study on the surface roughness characterization based on AFM measurements and fractal analysis.

FRACTAL ANALYSIS

Fractal analysis is a resolution analysis that tracks the recurrence of topographical surface at different length scales (17). Traditional Euclidean geometry depicts a perfect straight line, an ideal plane, and an ideal cube as 1-D, 2-D, and 3-D features, respectively. All these dimensions are topological and straightforward. For a much rugged line such as a coastline, however, its length critically depends on the size of a measuring ruler. As the resolution to look at the coastline is increased, i.e., the ruler size to measure the length is decreased, the length of the coastline is increased without an upper limit. Quite often

[1] Purdue University, School of Pharmacy, West Lafayette, Indiana 47907.

[2] To whom correspondence should be addressed. (e-mail: esp@omni.cc.purdue.edu)

0724-8741/98/0800-1222$15.00/0

one can observe the self-similarity of a coastline. The self-similarity is a property that part of the curve (or surface) is indistinguishable from the whole. The shape of the whole curve repeats even on a tiny part and the repeatability can be observed at all resolution levels. If a straight line is cut into M segments of the same size, the linear size of each segment is reduced by M fold. On the other hand, if a curve can be cut into M pieces of the same linear size, the linear size of each piece is reduced by $M^{1/D}$ fold. This curve is called a fractal, and the D value is called a fractal dimension which can be calculated to characterize its self-similarity.

For a rugged surface, which can be regarded between a smooth plane and a fully filled cube, fractal analysis can be used to evaluate the roughness. Fractal dimension is a universal number that can be used for numerical evaluation of the degree of surface irregularity or the space-filling ability. Because fractal dimension is an intrinsic feature of a fractal object, the fractal analysis is a perfect tool to characterize the lateral dimension and thus it is becoming a widely accepted approach to evaluate surface roughness (14,18,19). There are many methods to calculate fractal dimension of a rough surface. One method is based on the number of balls or boxes needed to cover the surface as the size of the ball or box is decreased (17). This method, called "box-counting method", computes fractal dimension from the relation between the number and the size of boxes. Fractal dimension can be defined based on the Minkowski-Bouligand denotation (20–22):

$$\Delta(E) = \lim_{\varepsilon \to 0} \left(3 - \frac{\log (V(E(\varepsilon))}{\log \varepsilon}\right) \quad (1)$$

where E is a bounded set in Euclidean space, and $E(\varepsilon)$ is set of all points within ε distance from E. $E(\varepsilon)$ is called the Minkowski sausage. Since $V(E(\varepsilon))$ is hard to evaluate and the Minkowski sausage is equivalent to the union of all the balls with radii ε centered on E, an approximation can be achieved using union of cubes (side length of ε) to cover E. Thus, fractal dimension can be calculated by the following definition:

$$\Delta(E) \approx \lim_{\varepsilon \to 0} \frac{\log \Omega_\varepsilon}{\log(1/\varepsilon)} \quad (2)$$

where Ω_ε is the number of cubes. This box-counting method, however, has been shown to be unsuitable for calculation of fractal dimensions from the digitized data (21). Calculation of fractal dimension by the power spectrum method (23,24) has also been shown to be unsuitable, since it generates relatively low-precision fractal dimensions (21). Recently, a much more robust method, known as the variation method, has been developed (20–22,25). The variation method uses a different approach to represent the Minkowski sausage. If the supremum, $v_f(x, y, \varepsilon) = sup\ |f(x_1, y_1) - f(x_2, y_2)|$, is taken over all the points such as $\max(|x - x_1|, |x - x_2|, |y - y_1|, |y - y_2|) \leq \varepsilon$, then the fractal dimension can be computed from integration of the supremums over all the points on the surface:

$$\Delta(E) = \lim_{\varepsilon \to 0} \left(3 - \frac{\log \int_x \int_y v_f(x, y, \varepsilon)\, dxdy}{\log \varepsilon}\right) \quad (3)$$

One of its useful features is that this method is not affected by an affine transformation of the amplitude. Let $Z = f(x, y)$ be a continuous function. For a constant C, f and Cf (affine transformation) should have exactly the same fractal dimension values. It has been demonstrated that the box-counting method is affected by an affine transformation but the variation method is not, even with the discrete digitized data (20,21).

EXPERIMENTAL

Materials

Caffeine (anhydrous powder, USP, Knoll AR, Ludwigshafen, Germany), chlorpheniramine maleate (USP, Schering-Plough, Kenilworth, NJ), lactose (hydrous, capsulating grade, Sheffield Products, Norwich, NY), hydroxypropyl methylcellulose (HPMC) (Methocel, K100M, The Dow Chemical, Midland, MI), ethylcellulose (EC) (Ethocel, 7FP, The Dow Chemical, Midland, MI), and, cellulose acetate phthalate (CAP) (Eastman Chemical Products, Kingsport, TN) were used for wet granulation. Dibasic calcium phosphate dihydrate (Di-Tab, USP, Rhône-Poulenc, Cranbury, NJ), croscarmellose sodium (Ac-Di-Sol, NF, FMC, Newark, DE), microcrystalline cellulose (Avicel, PH101, NF, FMC, Newark, DE) and mannitol (AR, Mallinckrodt Baker, Paris, KY) were used as received.

Samples for Fractal Measurements

Four wet granule samples were obtained from Dr. Garnet Peck at School of Pharmacy, Purdue University. The four samples were prepared using the following compositions: [1] caffeine (171.43 g), lactose (257.14 g), HPMC (114.29 g), CAP (28.57 g), EC (28.57 g), and wetting solvent (300 ml); [2] caffeine (171.43 g), lactose (257.14 g), HPMC (51.14 g), CAP (51.14 g), EC (51.14 g), and wetting solvent (155 ml); [3] chlorpheniramine maleate (171.43 g), lactose (257.14 g), HPMC (114.29 g), CAP (28.57 g), EC (28.57 g), and wetting solvent (300 ml); and [4] chlorpheniramine maleate (171.43 g), lactose (257.14 g), HPMC (51.14 g), CAP (51.14 g), EC (51.14 g), and wetting solvent (155 ml). The wetting solvent was prepared with acetone, ethanol, and water in the volume ratio of 20:20:1. Each sample was prepared by screening all ingredients with a 40-mesh sieve and then weighed. Drugs, polymers, and lactose were mixed with a V-shape blender for 10 min. Powders were transferred to a planetary mixer and sprayed with the wetting solution to make wet granules. The wet mass was screened with a 10-mesh sieve, and wet granules were dried in a hot air oven at 60°C overnight. Dried granules were screened with a 20-mesh sieve.

Di-Tab, Ac-Di-Sol, and Avicel were used as received to measure surface profiles. The fractal dimension values of mannitol powders were analyzed before and after freeze-drying. Freeze-dried mannitol powders were provided by Dr. Steven Nail at School of Pharmacy, Purdue University. The first set of mannitol samples (10% w/w) were prepared by freezing (at shelf temperature of −45°C for 6 hours), followed by primary drying (at −25°C for 48 hours under chamber pressure of 100 mTorr) and then secondary drying (at 25°C for 12 hours under 100 mTorr) in an FTS Dura-Stop freeze-drier (FTS System, Stone Ridge, NY). The second set of mannitol samples (10% w/w) were prepared by mixing with a red dye (0.5% w/w), Amaranth Red (Fisher Scientific, Pittsburgh, PA), followed by freeze-drying. The only difference in freeze-drying was that the primary drying took 60 hours. After freeze-drying, powders

were obtained by breaking the freeze-dried cakes with a spatula (the first set), or by hand shaking vials (the second set).

Atomic Force Microscopy

An atomic force microscope (AFM) used in our study was a NanoScope IIIa Multi-Mode AFM from Digital Instruments Inc. (Santa Barbara, CA). AFM scans were carried out in TappingMode with silicon probes which had the spring constants from 42.0 to 58.7 N/m. Resolution of all measurements was 512 × 512 points with equal steps along the x and y directions. Two scanners were used in our study: E scanner with 10 μm lateral and 2.5 μm vertical ranges; and J scanner with 125 μm lateral and 5 μm vertical ranges. The digital data were saved and converted to the plain text format that could be read by computer programs developed in our laboratory to calculate fractal dimension based on the variation method.

Implementation of the Variation Method

Implementation of the variation method was done on an IBM RISC/6000 workstation. The code was written in ANSI C. A PC version of the program is also available. To verify the correctness and to tune the heuristic parameters of the variation method, our program was tested using model surfaces with known theoretical or true fractal dimension values. The model surfaces were generated by fractional Brownian motion (26). Additional programs were also developed to visualize computer graphics of surface profiles. All the 3-D computer graphics in Figs. 1–5 were rendered and produced on workstations with our visualization programs.

RESULTS

Implementation of the Variation Method

Figure 1 shows four surface models with the theoretical fractal dimension values ranging from 2.2 to 2.8. Increase in surface roughness is obvious as the fractal dimension increases. Some of our test results are listed in Table 1. Table 1 clearly shows that our programs implementing the variation method are able to calculate fractal dimensions close to the theoretical values. An exception was observed when the surface roughness was extremely high, i.e., when fractal dimension values were large. When the theoretical values were 2.8 and 2.9, the calculated values were 2.73 and 2.79, respectively. A large difference could also be observed when the surface roughness was very low (i.e., 2.16 for 2.1). Although the calculated values of fractal dimension had relatively poor precision for both extremely rough and extremely smooth surfaces, the calculated values were monotonically increased as the true values increased. This particular feature indicates that the algorithm used is acceptable (22). Because extremely rough solid pharmaceutical materials are rare (as we have found out), we believe our programs are suitable for routine applications, especially when the fractal dimensions are 2.7 and smaller. Table 1 also shows that the calculated fractal dimension became closer to the theoretical value as the model size was increased from 257 × 257 to 1025 × 1025. One important conclusion from Table 1 is that affine transformations did not affect calculation of fractal dimension. The affine transformation was demonstrated by changing the initial standard deviation when generating a surface model (26).

In calculating fractal dimensions by the variation method, properly choosing heuristic parameters is very important (27). The variation method in the literature describes a heuristic

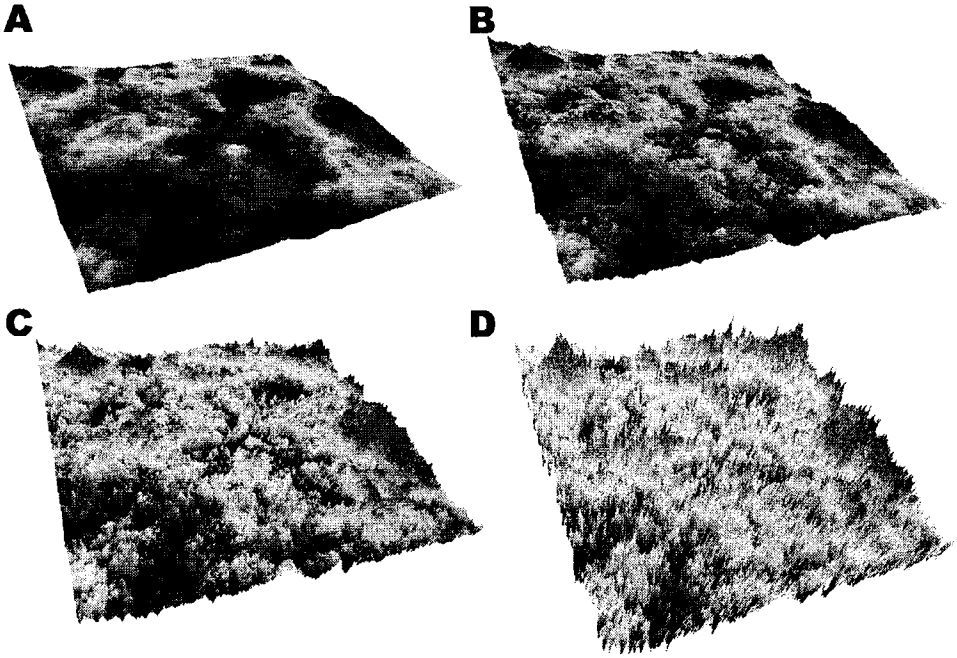

Fig. 1. Fractal surface models with different fractal dimension values generated by fractional Brownian motion. The fractal dimension values are 2.2 (A), 2.4 (B), 2.6 (C), and 2.8 (D). As the fractal dimension increases, the surface roughness also increases dramatically.

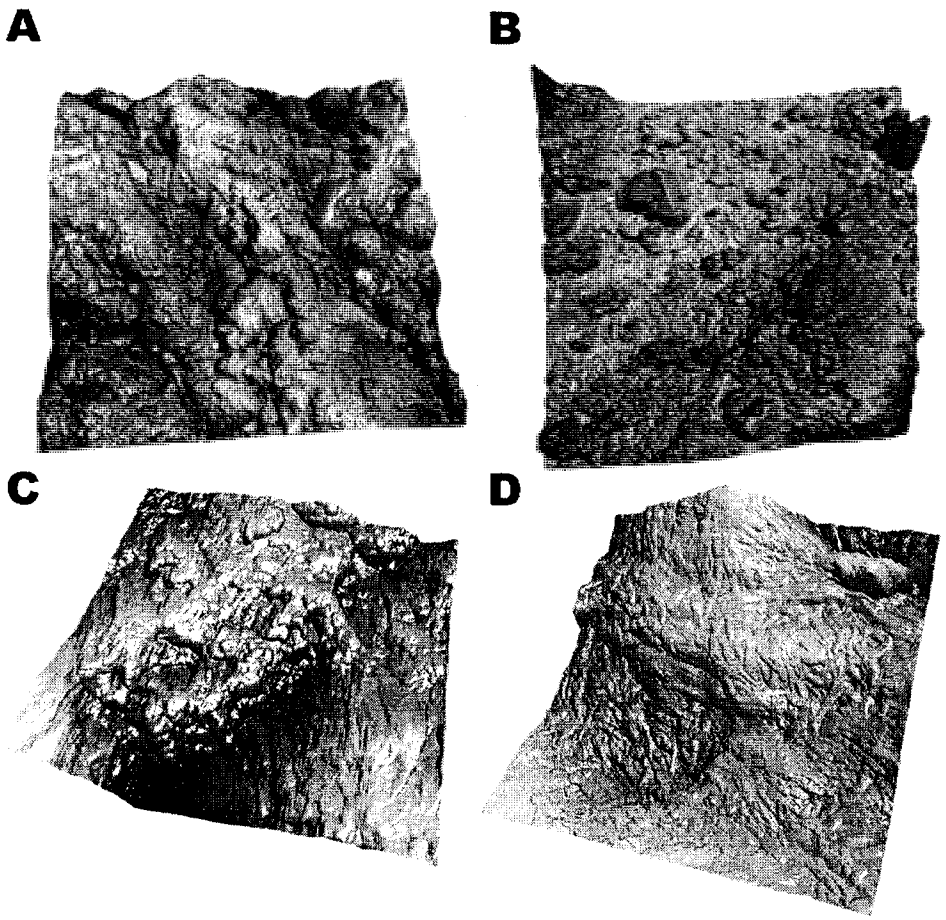

Fig. 2. 3-D rendered graphics of surfaces measured with AFM of wet granule (caffeine with HPMC, CAP and EC in 1:1:1 w/w ratio) (A), Di-Tab powder (B), Ac-Di-Sol powder (C), and Avicel PH101 powder (D). The fractal dimension values and scanning areas are 2.25 and 5 × 5 μm (A), 2.23 and 4 × 4 μm (B), 2.14 and 2 × 2 μm (C), and 2.13 and 2 × 2 μm (D), respectively.

parameter, R_{opt}, which is critical in the computation of the best value of fractal dimension (20,21). The essence of the variation method is to use bins as the basic unit instead of original data points to evaluate the supremum. This approach can largely improve the calculations. Reorganization of the N^2 points into R^2 bins (i.e., choosing a good R value) is the key to finding a precise fractal dimension value. The best R value, R_{opt}, is chosen from all possible values to have the smallest error in the linear fit of the log-log plot for calculation of the fractal dimension (i.e., $\log \int_x \int_y \nu_f(x, y, \varepsilon)\, dxdy$ versus $\log(\varepsilon)$, as in Equation 3) (20,21). Nevertheless, from testing fractal surface models with known theoretical fractal dimensions, we have found that the range for finding the best bin size, R_{opt}, should be different for surfaces with different roughness. For highly smooth surfaces (i.e., fractal dimension <2.2), the range to choose the best bin size, R_{opt}, is very narrow, starting from 1 data point and ending just after a few increases. On the other hand, for extremely rough surfaces (i.e., fractal dimension >2.7), the starting R has to be very large (e.g., 30 points) and a large range has to be scanned. For those surfaces with medium roughness, choices of the starting R and the scanned range are between the two extreme cases. Consequently, a self-adjusted approach is used in our programs. When computing an input surface profile, the programs first use a small range and a small starting bin size to find R_{opt}. If the calculated fractal dimension is bigger than the first threshold (e.g., 2.2), the programs calculate again with a medium range and a medium starting bin size. If a fractal dimension value is still bigger than the second threshold (e.g., 2.5), the programs use a large range and a large starting bin size for the calculation. All the values of bin ranges and starting bin sizes have to be tuned with surface models with known theoretical or true fractal dimensions to get the best results.

Because of the usage of heuristic parameters such as the bin range and starting bin size in determining fractal dimension, there would be differences introduced between the true and calculated fractal dimension values of real surfaces. In addition, a small change of heuristic parameters can induce a relatively large change in the estimation of fractal dimensions. For the same surface, different algorithms could yield different fractal dimension values. Even the same algorithm could give different values with different implementations. Therefore, the true fractal dimension value of a surface would never be known due to the involvement of heuristic parameters in all algorithms used for calculation of fractal dimension. This, however, does not mean that the calculated fractal dimension values are of little value. A good algorithm should give monotonically increased

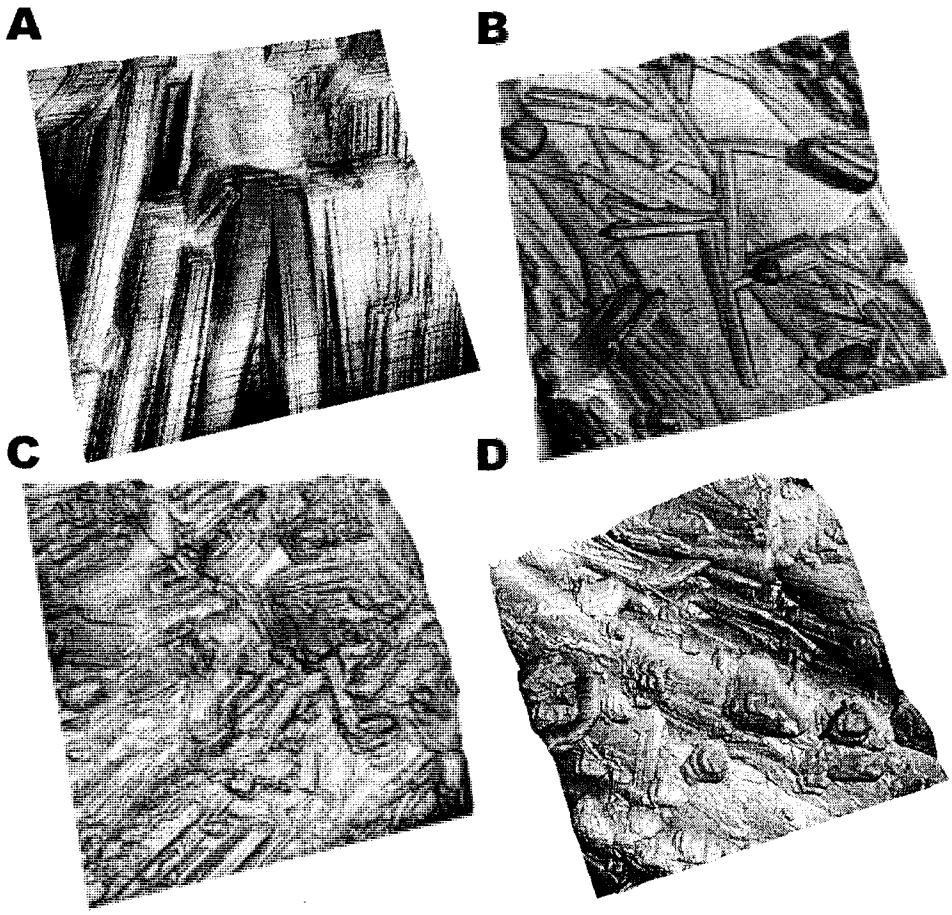

Fig. 3. 3-D rendered graphics of surfaces measured with AFM of four mannitol powder samples. Fractal dimension values are (A) 2.13 (1 × 1 μm scanning), (B) 2.16 (5 × 5 μm scanning), (C) 2.16 (15 × 15 μm scanning), and (D) 2.15 (20 × 20 μm scanning), respectively.

fractal dimension values when the true values increase so that the computed values can be used to correlate with other physical properties (22). Such an algorithm should also be robust and consistent. Our tests show the variation method has these desired features, and our programs run correctly.

It is necessary to point out that for the same theoretical fractal dimension, different surface models generated with different random number seeds could result in different calculated fractal dimension values. The calculated values can also be dependent on the number of data points of surface profiles. Nevertheless, the calculated values of surfaces with the same theoretical fractal dimension are close to the true value with small deviations. This indicates that the fractal dimension calculated from either a surface model or a real solid surface profile follows a statistical distribution. The calculated fractal dimension values are distributed in some form centering on the true or real value. Thus, the average value of fractal dimension is expected to represent the true value.

Fractal Analysis of Pharmaceutical Samples

Surface profiles of four wet granule samples, Di-Tab, Ac-Di-Sol, Avicel, and mannitol powders were measured with an AFM and analyzed with our fractal analysis programs. For each sample, many AFM measurements were carried out on different particles and on different areas of a same particle. The 3-D computer graphics of some surface profiles are shown in Figs. 2–5. The results of fractal dimension values, including the average values, maximum calculated values, and minimum calculated values, are listed in Table 2. Average height values of all surfaces measured are also listed in the table. The lowest point of every surface profile was taken as the bottom level to calculate the height of each point. The correlation coefficient square of the linear curve fitting for calculation of any fractal dimension (i.e., $\log \int_x \int_y \nu_f(x, y, \varepsilon)\, dxdy$ versus $\log(\varepsilon)$, as in Equation 3) listed in Table 2 was at least 0.99.

Figure 2 shows 3-D surface images of a wet granule sample, Di-Tab, Ac-Di-Sol, and Avicel PH101. Although the first two surface profiles (Figs. 2-A and B) had a little larger fractal dimension values than the last two (Figs. 2-C and D), the average calculated values of fractal dimension of these four systems and other three wet granule samples were close to each other. These images demonstrate that AFM is able to gather 3-D surface profiles at the nanoscale. These detailed, highly resolved 3-D surface data allow accurate fractal analysis. The only limitation we noticed in our study was the short vertical range (2.5 μm or 5.0 μm) of the AFM scanners. This limitation makes it difficult to measure large surface areas because the surface height could be out of the measuring range. These

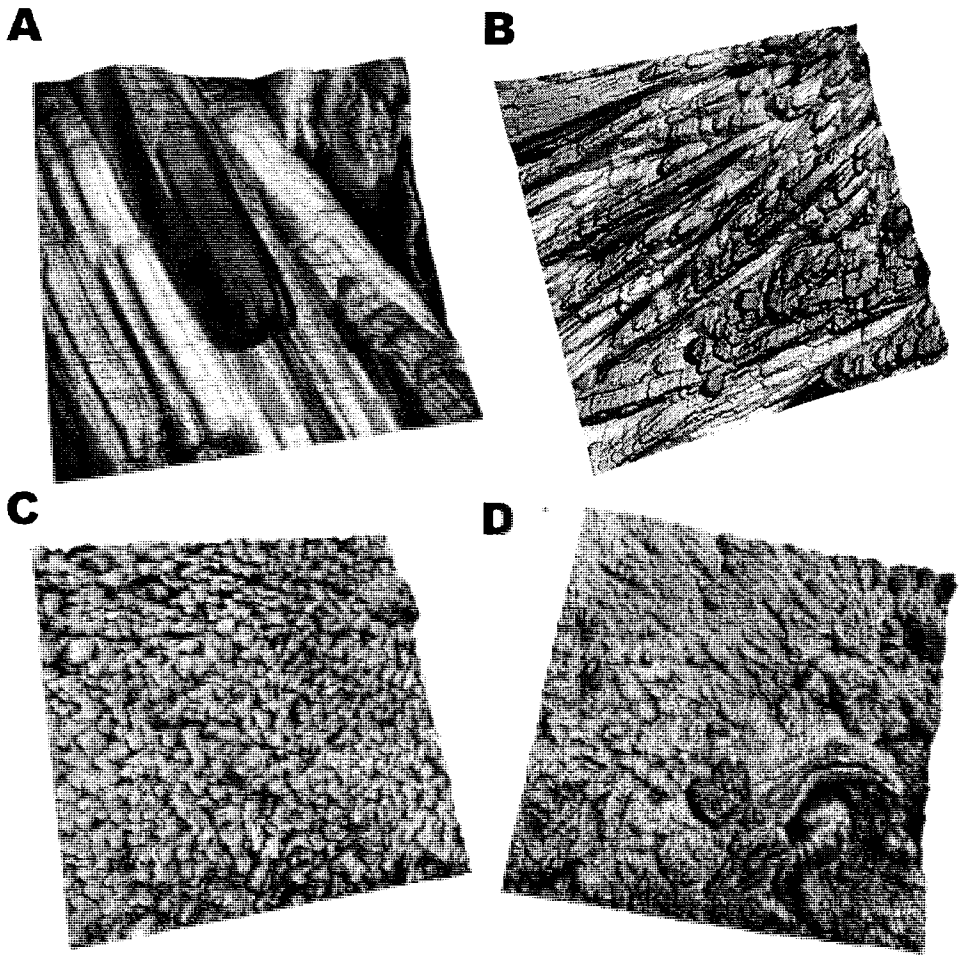

Fig. 4. 3-D rendered graphics of surfaces measured with AFM of four freeze-dried mannitol powder samples. Fractal dimension values are (A) 2.11 (1 × 1 μm scanning), (B) 2.33 (10 × 10 μm scanning), (C) 2.48 (20 × 20 μm scanning), and (D) 2.36 (20 × 20 μm scanning), respectively.

surface data also made it easy to directly visualize the surface textures in 3-D. Fig. 2-D shows an interesting texture of Avicel. The "fiber"-looking features on the Avicel surface could be the individual microcrystals.

Figures 3–5 show surface graphics of bulk mannitol, freeze-dried mannitol, and freeze-dried mannitol with the dye, respectively. Four images of different scan areas are shown for each sample. After freeze-drying, the mannitol surface became very different, i.e., much rougher, and the fractal dimension became significantly larger. In addition, the surface texture appeared to be changed by the freeze-drying process. Fig. 3 shows needle-shaped mannitol crystals on the surfaces while no such mannitol crystals were observed on the freeze-dried mannitol surfaces (Figs. 4 and 5). The presence of tiny grains made the surface much more irregular. Again, these images showed the AFM's ability to probe and obtain 3-D surface profiles at the nanoscale. For example, Fig. 5-A shows detailed features of a 1 × 1 μm area of the freeze-dried mannitol with the dye.

Table 2 shows fractal dimension values of four wet granule samples, Di-Tab, Ac-Di-Sol, Avicel PH101, and mannitol bulk powders. Fractal dimension values of all samples were small and close to each other. The average values were in a very narrow range from 2.06 to 2.17. For powder samples, different scan areas were tested and the effect of the scan area on fractal dimension was studied. It was shown that the scan size in the range we studied had little influence on the fractal dimension of raw powder materials. Regardless of the scan size, the average values of Di-Tab, Ac-Di-Sol, Avicel, and mannitol were 2.14 ± 0.04, 2.12 ± 0.03, 2.12 ± 0.04, 2.11 ± 0.04, respectively. Surfaces of these samples were not rough and the surface roughness did not depend on the scan area. It was interesting to observe that the results of freeze-dried mannitol powders (with and without the dye) were quite different. Their fractal dimension values were larger than those of control samples and varied with different scan areas. Fig. 6 shows fractal dimension as a function of the scan size (which is the square root of the scan area) of Di-Tab, mannitol powders, freeze-dried mannitol, and freeze-dried mannitol mixed with the dye. As shown in Fig. 6, fractal dimension values of Di-Tab and bulk mannitol powders did not change very much as the scan size increased. The standard deviations of these two systems were also small. The fractal dimension was usually smaller than 2.20 regardless of the scan size. The maximum values calculated for Di-Tab and mannitol powders were 2.26 and 2.20, respectively. On the other hand, for the two freeze-dried mannitol powders, the

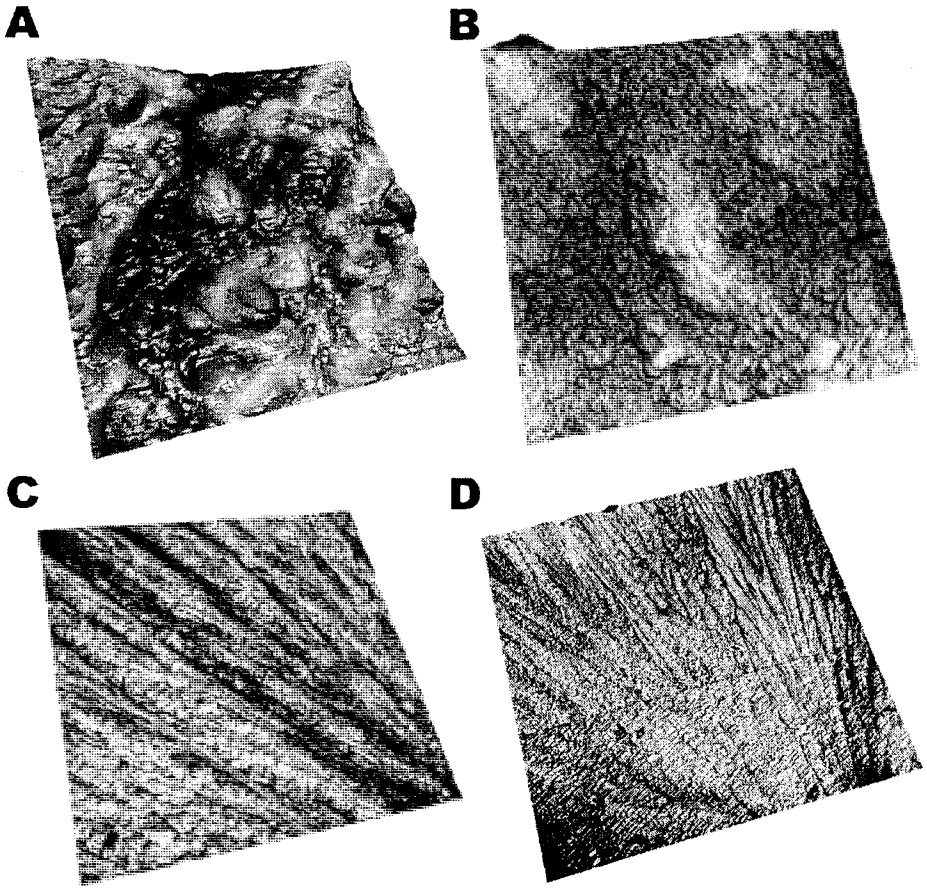

Fig. 5. 3-D rendered graphics of surfaces measured with AFM of four powder samples of freeze-dried mannitol and a dye. Fractal dimension values are (A) 2.18 (1 × 1 μm scanning), (B) 2.34 (5 × 5 μm scanning), (C) 2.52 (10 × 10 μm scanning), and (D) 2.47 (40 × 40 μm scanning), respectively.

fractal dimension value changed significantly as the scan size increased. The standard deviation was significantly larger, especially for the freeze-dried mannitol mixed with the dye. Increase of fractal dimension of the first set of freeze-dried mannitol samples was apparent as the scan size became larger as shown in Fig. 6. For the second set of freeze-dried mannitol samples, the fractal dimension changed more dramatically as the scan size increased. At the scan size of 10 μm, fractal dimension already reached the highest value of 2.52, with the average of 2.31. Above this scan size, fractal dimension varied with large standard deviations without any noticeable trend. For the two sets of freeze-dried mannitol powders, fractal dimension increased from a small value of about 2.1 at 0.5 μm or 1.0 μm scan size to a large value of about 2.3 at 10 μm scan size. Table 2 also lists the average height of surface profiles measured with AFM. It was generally shown that the average height increased as the scan size increased. It appeared that there was no clear relationship between the average height and the fractal dimension.

DISCUSSION

It is interesting to notice that fractal dimensions of wet granules and raw powder materials (Di-Tab, Ac-Di-Sol, Avicel, and mannitol) were small and close to each other. The average fractal dimension values were generally smaller than 2.20. In addition, fractal dimensions of these samples were not related to the scan size or scan area in the range we measured. Nevertheless, fractal dimensions of two freeze-dried mannitol samples showed strong dependence on the scan size. Most significantly, fractal dimensions were larger than those of wet granules and raw powder materials. Surfaces of freeze-dried mannitol became much more rugged. The largest fractal dimension values were 2.48 for the first set of samples and 2.52 for the second set as seen in Table 2, respectively. Apparently, the freeze-drying process changed the surface morphology of mannitol and rendered the surface more coarse. Considering that the raw materials are prepared mechanically during their last production processes (such as milling, cutting, sieving, compaction, etc.), we can expect that the mechanical processes smoothen local areas of these materials so their fractal dimensions are smaller than 2.20 for the samples used in this study. Of course, we are not sure whether at larger scales (i.e., larger scan sizes), such as millimeter or ever larger, fractal dimensions of these raw materials become much different (i.e., either bigger or smaller). This study showed that AFM was able to probe differences of the surface morphology or texture caused by a physicochemical process such as freeze drying. A physicochemical process occurs at the molecular level so that the impact on surface

Table 1. Theoretical and Calculated Fractal Dimension Values of Fractal Surfaces Generated by Fractional Brownian Motion

Theoretical Fractal Dimension	Model Size[a]	Initial Standard Deviation[b]	Calculated Fractal Dimension[c]
2.1	513 × 513	50	2.16 ± 0.03
2.2	513 × 513	50	2.24 ± 0.04
2.3	513 × 513	50	2.32 ± 0.03
2.4	513 × 513	50	2.40 ± 0.04
2.5	513 × 513	50	2.48 ± 0.02
2.6	513 × 513	50	2.62 ± 0.05
2.7	513 × 513	50	2.68 ± 0.04
2.8	513 × 513	50	2.73 ± 0.03
2.9	513 × 513	50	2.79 ± 0.02
2.1	257 × 257	50	2.15 ± 0.03
2.3	257 × 257	50	2.32 ± 0.03
2.5	257 × 257	50	2.45 ± 0.02
2.7	257 × 257	50	2.67 ± 0.05
2.9	257 × 257	50	2.76 ± 0.03
2.1	1025 × 1025	50	2.17 ± 0.03
2.3	1025 × 1025	50	2.32 ± 0.03
2.5	1025 × 1025	50	2.50 ± 0.06
2.7	1025 × 1025	50	2.69 ± 0.04
2.9	1025 × 1025	50	2.80 ± 0.02
2.3	513 × 513	10	2.32 ± 0.03
2.3	513 × 513	30	2.32 ± 0.03
2.3	513 × 513	200	2.32 ± 0.03
2.5	513 × 513	10	2.48 ± 0.03
2.5	513 × 513	30	2.47 ± 0.03
2.5	513 × 513	200	2.47 ± 0.03
2.7	513 × 513	10	2.69 ± 0.04
2.7	513 × 513	30	2.68 ± 0.04
2.7	513 × 513	200	2.69 ± 0.04

[a] Model size shows the number of points along X and Y. The distance between consecutive points along X and Y was chosen as 8, 4, 2 for model size 257 × 257, 513 × 513, and 1025 × 1025, respectively.
[b] Initial standard deviation defines the average height of a surface model.
[c] For each test, 10 different surfaces were tested by using 10 different random-number generation seeds.

morphology including surface roughness can be observed with AFM. On the other hand, since most mechanical equipment and workpieces are large, their impact on the surface morphology is macroscopic and may be beyond the measuring range of AFM. It is speculated that at larger scales wet granules and raw powders may show significant differences in their fractal features.

The relationship between fractal dimension and observation scale is thought to depend on the way that surface was formed. A surface feature or morphology is caused by certain processes, either mechanical or physicochemical, and such processes may act separately or simultaneously. The scale of influences by such processes can be very small (in the angstrom or nanometer scale) or very large (in the millimeter or meter scale). Furthermore, influence on the surface morphology can be homogeneous or heterogeneous. Thus, the surface morphology could be very simple or very complicated. Since fractal dimension defines the space-filling ability of a surface, it can be used to reflect or retrace the influence of the processes that produced the material's surface. It is well known that a pure fractal generated with mathematical functions has a single fractal dimension value regardless of the observation scale. The reason is apparent. The mechanism to form the fractal is isotropic and is not scale-dependent. Thus, if a physicochemical process is isotropic (i.e., not scale-dependent) and it is the only mechanism to form a surface, fractal dimension of this surface is constant regardless of the observation scale. One example is simulated snowflakes formed by diffusion-limited aggregation (28,29). For most materials, however, fractal dimension is scale-dependent and not homogeneous because of different processes influencing the surface at different scales. The interplay of different influences results in a heterogeneous surface morphology. Therefore, fractal dimension may be not only scale-dependent, but also different on different spots on the surface, i.e., a single fractal dimension value may not be used to characterize the entire surface because it is a composite of fractals of different dimensions (multifractal). The observation that fractal dimension of wet granules and raw powder materials were similar at the scales from 0.5 to 20 μm (see Table 2) indicates that mechanical processes undermine the influences of the material's compositions and chemical identities. Although their fractal dimension values were small, we may expect that different results could be obtained at larger scales, such as hundred micrometers or larger. We observed a rather dramatic influence of the freeze-drying process on surface morphology. Large standard deviations indicate that the influence or impact of freeze-drying was anisotropic on the surface. In addition, the second set of freeze-dried samples showed larger standard deviations. Different spots showed different fractal features. Either different form of mannitol crystals and/or the presence of the dye affected the formation of surface morphology. The direct relationship between fractal dimension and the underlying physical process was reported by others as well (30).

The average height shown in Table 2 revealed another aspect of surface roughness. However, there was no apparent relationship between the height and fractal dimension. There was also no apparent influence of the freeze-drying process on the average height of mannitol samples. Moreover, large standard deviations of the average height indicate that the height distribution on surfaces was heterogeneous. Fractal dimension reflected the impact of freeze-drying while height did not, and this may be due to the way in which they were computed. Although both fractal dimension and height are necessary to describe surface roughness, the fractal dimension is much more sensitive to changes of surface morphology, and in fact, fractal dimension alone can be used to represent the surface roughness. Since fractal analysis can provide a quantitative parameter representing the surface roughness, it can be a valuable tool for surface characterization of pharmaceutical particles.

CONCLUSIONS

We implemented the variation method for calculation of fractal dimension and fractal analysis was applied to characterization of pharmaceutical solid materials based on AFM measurement. The variation method is shown to be most suitable for carrying out fractal analysis. Yet, implementation of the method needs careful and extensive adjustments of heuristic parameters. This was achieved using the theoretical surface models generated by fractional Brownian motion with

Table 2. Fractal Analysis of Pharmaceutical Samples

Measured Sample	Scanning Area (μm^2)	Tests #[a]	Average FD ± SD	Max. FD[b]	Min. FD[b]	Average Height ± SD[c]
Granule of caffeine with HPMC, CAP and EC in 4:1:1 w/w ratio	5 × 5	9	2.16 ± 0.04	2.22	2.09	1.00 ± 0.28
Granule of caffeine with HPMC, CAP and EC in 1:1:1 w/w ratio	5 × 5	9	2.15 ± 0.04	2.25	2.10	0.90 ± 0.23
Granule of chlorpheniramine maleate with HPMC, CAP and EC in 4:1:1 w/w ratio	5 × 5	13	2.12 ± 0.03	2.17	2.08	0.84 ± 0.28
Granule of chlorpheniramine maleate with HPMC, CAP and EC in 1:1:1 w/w ratio	5 × 5	9	2.13 ± 0.06	2.25	2.08	0.93 ± 0.42
Di-Tab (dibasic calcium phosphate Dihydrate)	0.5 × 0.5	15	2.10 ± 0.04	2.19	2.06	0.12 ± 0.08
	1 × 1	21	2.14 ± 0.05	2.24	2.06	0.23 ± 0.10
	2 × 2	4	2.14 ± 0.04	2.18	2.10	0.41 ± 0.04
	3 × 3	7	2.14 ± 0.06	2.24	2.08	0.73 ± 0.30
	4 × 4	9	2.16 ± 0.04	2.24	2.12	0.92 ± 0.35
	5 × 5	11	2.15 ± 0.04	2.26	2.10	1.16 ± 0.43
	10 × 10	6	2.14 ± 0.01	2.16	2.13	1.94 ± 0.78
	15 × 15	2	2.14	2.15	2.12	3.57
Ac-Di-Sol (croscarmellose sodium)	1 × 1	11	2.12 ± 0.03	2.16	2.07	0.18 ± 0.21
	2 × 2	7	2.12 ± 0.03	2.17	2.09	0.25 ± 0.10
	3 × 3	2	2.08	2.10	2.06	0.51
Avicel PH101 (microcrystalline cellulose)	1 × 1	16	2.12 ± 0.05	2.24	2.03	0.24 ± 0.05
	2 × 2	8	2.12 ± 0.03	2.15	2.07	0.38 ± 0.11
	3 × 3	1	2.15			0.62
Mannitol powders	1 × 1	8	2.10 ± 0.03	2.13	2.05	0.086 ± 0.045
	2 × 2	1	2.06			0.31
	3 × 3	3	2.11 ± 0.06	2.18	2.06	0.34 ± 0.05
	5 × 5	16	2.10 ± 0.04	2.20	2.05	0.87 ± 0.43
	10 × 10	13	2.12 ± 0.03	2.16	2.08	1.84 ± 0.82
	15 × 15	3	2.13 ± 0.03	2.16	2.09	1.65 ± 0.10
	20 × 20	3	2.17 ± 0.02	2.20	2.15	1.39 ± 0.52
Freeze-dried mannitol powders	1 × 1	8	2.08 ± 0.02	2.11	2.05	0.14 ± 0.05
	5 × 5	17	2.17 ± 0.07	2.30	2.06	0.56 ± 0.29
	10 × 10	16	2.25 ± 0.07	2.34	2.13	0.78 ± 0.57
	15 × 15	5	2.33 ± 0.03	2.36	2.30	0.85 ± 0.53
	20 × 20	5	2.36 ± 0.07	2.48	2.30	1.09 ± 0.64
	30 × 30	1	2.47			3.66
Freeze-dried mannitol with a dye	0.5 × 0.5	5	2.13 ± 0.03	2.16	2.10	0.071 ± 0.050
	1 × 1	13	2.12 ± 0.06	2.27	2.05	0.10 ± 0.06
	5 × 5	20	2.24 ± 0.09	2.38	2.12	0.41 ± 0.38
	10 × 10	19	2.31 ± 0.11	2.52	2.12	0.56 ± 0.79
	15 × 15	6	2.30 ± 0.06	2.36	2.23	0.43 ± 0.24
	20 × 20	6	2.33 ± 0.09	2.45	2.18	0.62 ± 0.42
	30 × 30	3	2.22 ± 0.12	2.36	2.14	1.86 ± 1.40
	40 × 40	1	2.47			0.39
	50 × 50	1	2.30			1.72

[a] Test # is the number of samples tested.
[b] Maximum and minimum fractal dimensions (FD) are those found among all calculated values in a given system.
[c] The average height (in μm) is relative to the lowest point of each measurement.

known fractal dimensions. AFM has demonstrated its ability to measure 3-D surface profiles at the nanoscale. Our results of fractal analysis of four wet granule samples, raw powder materials (Di-Tab, Ac-Di-Sol, Avicel PH101, and mannitol), and freeze-dried mannitol powders revealed an intrinsic relationship between fractal dimension and underlying processes which produced the material and formed the surface morphology. Our method not only showed a way to quantify the surface roughness, but also indicated the importance of the observation scale for studying the surface morphology and roughness. Nanoscale measurements with AFM are able to reveal influences of the underlying physicochemical processes occurring at the molecular level. For the mechanically processed materials, however, larger-scale measurements may have to be used. Studies of the relationship between surface roughness and physicochemical properties of a material require

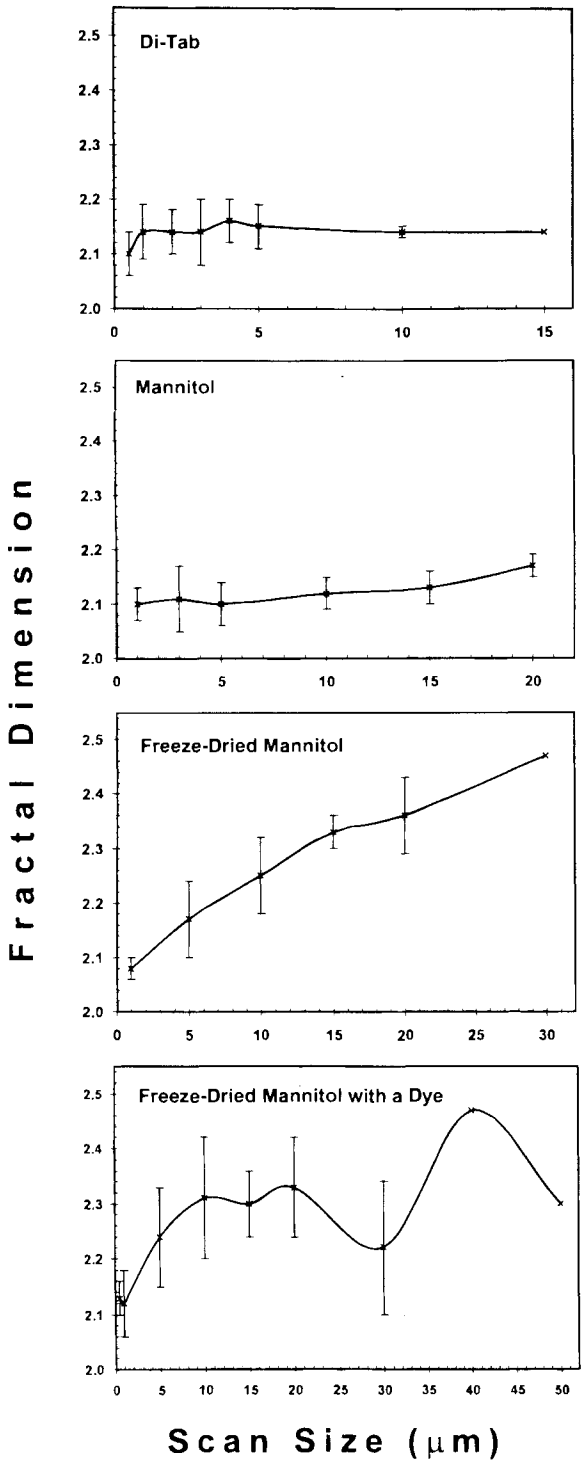

Fig. 6. Fractal dimension values of four different samples as a function of the scan size. Since AFM scanning area was square, scan size indicates the length of one side of the scanning area.

thorough measurements of fractal dimension values as a function of the observation scale.

ACKNOWLEDGMENTS

The authors would like to thank Dr. Garnet Peck and Phuriwat Leesawat for providing granule samples, and Dr. Steven Nail, Wei Liu and Alexandra Kim for providing freeze-dried mannitol samples. This project was supported by a grant from NSF Industry/University Cooperative Research Center in Pharmaceutical Processing at Purdue University.

REFERENCES

1. S. R. Byrn. *Solid State Chemistry of Drugs*, Academic Press, New York, 1982,
2. H. G. Brittain, S. J. Bogdanowich, D. E. Bugay, J. DeVincentis, G. Lewen, and A. W. Newman. Physical characterization of pharmaceutical solids. *Pharm. Res.* **8**:963–973 (1991).
3. M. A. Ramadan and R. Tawashi. Effect of surface geometry and morphic features on the flow characteristics of microsphere suspensions. *J. Pharm. Sci.* **79**:929–933 (1990).
4. P. D. Nadkarni, D. O. Kildsig, P. A. Kramer, and G. S. Banker. Effect of surface roughness and coating solvent on film adhesion to tablets. *J. Pharm. Sci.* **64**:1554–1557 (1975).
5. T. Oshima, Y.-L. Zhang, M. Hirota, M. Suzuki, and T. Nakagawa. The effect of the types of mill on the flowability of ground powders. *Adv. Powder Technol.* **6**:35–45 (1995).
6. C.-T. Lee and C. C.-K. Chou. Application of fractal geometry in quantitative characterization of aerosol morphology. *Part. Part. Syst. Charact.* **11**:436–441 (1994).
7. R. Thibert, M. Akbarieh, and R. Tawashi. Application of fractal dimension to the study of the surface ruggedness of granular solids and excipients. *J. Pharm. Sci.* **77**:724–726 (1988).
8. J. M. Bennett. Recent developments in surface roughness characterization. *Meas. Sci. Technol.* **3**:1119–1127 (1992).
9. R. M. Hall, A. Unsworth, P. Siney, and B. M. Wroblewski. The surface topography of retrieved femoral heads. *J. Mater. Sci. Mater. Med.* **7**:739–744 (1996).
10. T. Provder and B. Kunz. Application of profilometry and fractal analysis to the characterization of coatings surface roughness. *Prog. Org. Coat.* **27**:219–226 (1996).
11. S. R. Brown and C. H. Scholz. Broad bandwidth study of the topography of natural rock surfaces. *J. Geophys. Res.* **90**:12575–12582 (1985).
12. W. L. Power and T. E. Tullis. Euclidean and fractal models for the description of rock surface roughness. *J. Geophys. Res.* **96**:415–424 (1991).
13. B. B. Mandelbrot. *Fractals: Form, Chance, and Dimension*, W. H. Freeman, San Francisco, 1977,
14. D. Farin and D. Avnir. Reactive fractal surfaces. *J. Phys. Chem.* **91**:5517–5521 (1987).
15. B. H. Kaye. Characterizing the structure of fumed pigments using the concepts of fractal geometry. *Part. Part. Syst. Charact.* **8**:63–71 (1991).
16. F. Family, P. Meakin, B. Sapoval, and R. Wool (eds.). *Fractal Aspects of Materials*, Materials Research Society, Pittsburgh, 1995.
17. A. Seri-Levy and D. Avnir. Fractal analysis of surface geometry effects on catalytic reactions. *Surf. Sci.* **248**:258–270 (1991).
18. D. Avnir, D. Farin, and P. Pfeifer. Surface geometric irregularity of particulate materials: The fractal approach. *J. Colloid Interface Sci.* **103**:112–123 (1985).
19. Y. H. Lee, J. R. Carr, D. J. Barr, and C. J. Haas. The fractal dimension as a measure of the roughness of rock discontinuity profiles. *Int. J. Rock Mech. Min. Sci. Geomech. Abstr.* **27**:453–464 (1990).
20. B. Dubuc, S. W. Zucker, C. Tricot, J. F. Quiniou, and D. Wehbi. Evaluating the fractal dimension of surfaces. *Proc. R. Soc. Lond. A.* **425**:113–127 (1989).
21. B. Dubuc, J. F. Quiniou, C. Roques-Carmes, C. Tricot, and S. W. Zucker. Evaluating the fractal dimension of profiles. *Phys. Rev. A.* **39**:1500–1512 (1989).
22. B. Dubuc and S. Dubuc. Error bounds on the estimation of fractal dimension. *SIAM J. Number. Anal.* **33**:602–626 (1996).
23. S. Ganti and B. Bhushan. Generalized fractal analysis and its applications to engineering surfaces. *Wear* **180**:17–34 (1995).
24. A. Majumdar and B. Bhushan. Role of fractal geometry in roughness characterization and contact mechanics of surfaces. *J. Tribol.* **112**:205–216 (1990).
25. R. Thibert, B. Dubuc, M. Dufour, and R. Tawashi. Evaluation

of the surface roughness of cystine stones using a visible laser diode scattering approach. *Scanning Microsc.* **7**:555–561 (1993).
26. M. F. Barnsley, R. L. Devaney, B. B. Mandelbrot, H.-O. Peitgen, D. Saupe, R. F. Voss, Y. Fisher, and M. McGuire. *The Science of Fractal Images*, Springer-Verlag, New York, 1988.
27. Q. Huang, J. R. Lorch, and R. C. Dubes. Can the fractal dimension of images be measured? *Pattern Recognit.* **27**:339–349 (1994).
28. J. Nittmann and H. E. Stanley. Non-deterministic approach to anisotropic growth patterns with continuously tunable morphology: The fractal properties of some real snowflakes. *J. Phys. A.* **20**:L1185–L1191 (1987).
29. J. Kertész and T. Vicsek. Diffusion-limited aggregation and regular patterns: Fluctuations versus anisotropy. *J. Phys. A.* **19**:L257–L260 (1986).
30. J. C. Sommerer and E. Ott. Particles floating on a moving fluid: A dynamically comprehensible physical fractal. *Science* **259**:335–339 (1993).